ISSN 0016-8521, Geotectonics, 2014, Vol. 48, No. 2, pp. 122–138. © Pleiades Publishing, Inc., 2014.
Original Russian Text © A.I. Kozhurin, T.K. Pinegina, V.V. Ponomareva, E.A. Zelenin, P.G. Mikhailyukova, 2014, published in Geotektonika, 2014, Vol. 48, No. 2, pp. 42–60.

Rate of Collisional Deformation in Kamchatsky Peninsula, Kamchatka

A. I. Kozhurin[a], T. K. Pinegina[b], V. V. Ponomareva[b], E. A. Zelenin[a], and P. G. Mikhailyukova[c]

[a] *Geological Institute, Russian Academy of Sciences, Pyzhevskii per. 7, Moscow, 119017 Russia*
e-mail: anivko@yandex.ru
[b] *Institute of Volcanology and Seismology, Far East Branch, Russian Academy of Sciences, bul'v. Piipa 9, Petropavlovsk-Kamchatsky, 683006 Russia*
[c] *Faculty of Geography, Moscow State University, Moscow, 119234 Russia*

Received July 22, 2013

Abstract—Detailed data are discussed on the rate of Holocene horizontal and vertical movements along a fault in the southeastern Kamchatsky Peninsula, which is situated between the converging Aleutian and Kamchatka island arcs. The fault is the northern boundary of the block invading into the peninsula under pressure of the Komandorsky Block of the Aleutian arc. The rate of right-lateral slip along the fault was increasing in the Holocene and reached 18–19 mm/yr over the last 2000 years and 20 mm/yr by contemporary time. Comparison of these estimates with those that follow from offsets of older rocks also indicates acceleration of horizontal movements along the fault from the early Quaternary to the present. The results obtained from rates of GPS station migration show that about half the rate of the northwestern drift of the Komandorsky Block is consumed for movement of the block of the southern side of the fault. The remainder of movement of the Komandorsky Block is consumed for movements (probably, underthrusting) at the eastern continental slope of the Kamchatsky Peninsula.

Keywords: active fault, displacement rate, Kamchatka–Aleutian arc collision

DOI: 10.1134/S001685211402006X

INTRODUCTION

Interaction between each couple of neighboring island arcs in the northwestern Pacific Ocean—Izu–Bonin and Japan [15, 46], Japan and Kurile [31–33], Kamchatka and Aleutian [29]—develops according to the collisional scenario. The tangential component of oceanic plate motion, which appears under nonorthogonal underthrusting, is the driving force of arcs (more precisely, of their ends) convergence [22, 26]. Depending on the direction of oceanic plate motion, the value of the tangential component can be equal for two arcs, often unequal, and in the extreme case, relative motion is absent in one arc and accommodated in the other. The kinematic situation at the junction of the Aleutian and Kamchatka arcs corresponds to the latter variant. The Pacific Plate subducting beneath Kamchatka at almost an orthogonal angle moves parallel to the westernmost Komandorsky segment of the Aleutian arc (Fig. 1).

The rate of collisional deformation, i.e., the rate of lateral shortening of the Earth's crust in the collision zone is an important characteristic of this process. Its maximum value cannot exceed the tangential component of the rate of oceanic plate motion, and the real value shows what part of the total relative motion is transferred to island arc convergence and deformation in the collision zone.

The rate of Pacific Plate movement relative to the North American Plate near the northern end of the Kurile–Kamchatka subduction zone is about 8 cm/yr with a difference of a few millimeters between the NUVEL-1 and NUVEL-1a models [24, 25] and rate estimates based on space geodesy [23, 24, 44]. The displacements in the Komandorsky segment of the Aleutian arc are distributed over several longitudinal right-lateral strike-slip faults [12, 13, 16]. Taken together, they make up the so-called diffuse transform zone [21] with a decrease in the motion rate away from the Pacific Ocean [34]. According to GPS measurements, the present-day rate of the Komandorsky Block movement toward Kamchatka is approximately 55 mm/yr [14, 20], i.e., about two-thirds the rate of the Pacific Plate motion.

The Kamchatsky Peninsula is located between Kamchatka and the Aleutian arc behind the western end of the Aleutian Transform Fault, so that its deformations can be related only to stress from the Aleutian arc. The fast vertical movements and high rate of exhumation of pre-Pliocene rocks in the eastern part of the peninsula [27], formation of Pleistocene and Holocene marine terraces [11, 40–42], and move-

ments along active faults [1, 28] are considered as manifestations of collision.

The rate of collisional deformation of the peninsula and its relationships to the rate of northwestern drift of Komandorsky Block of the Aleutian arc are estimated in this paper based on the sense and average rate of movements along the near-latitudinal fault in the southeastern part of the peninsula. This fault, called below the Second Pereval'naya, is the northern limitation of the frontal part of the Komandorsky Block or a separate block in front of the latter. In the first version, this fault is interpreted as a branch of the Bering Fault [27, 28] (Figs. 2a, 2b), and in the second version, as a relatively independent structural element [8] (Fig. 2c).

The published estimates of the average lateral slip rate in the central part of the fault over the Holocene, which are based on single determinations of radiocarbon age of displaced landforms, are scattered from 15 to 20 mm/yr [6]. The slip rate at the western end of this fault, involving tephrochronological datings of the displaced river terrace, was estimated at 4 mm/yr [34].

In this paper, we report new data, which allowed us to obtain precise estimates of the average rates of vertical and horizontal movements along the Second Pereval'naya Fault. The measurements were carried out at two observation points along the fault line. In the near-shore zone, we have measured and dated vertical and horizontal displacements of late Holocene marine terraces and deformations of Holocene loose sediments in the trench excavated across the fault scarp. The largest of the observed displacements of erosion topography elements have been measured and dated in the central segment of the fault.

GENERAL CHARACTERIZATION OF THE SECOND PEREVAL'NAYA FAULT

The activity of the Second Pereval'naya Fault and its right-lateral kinematics were established long ago [6, 7]. The idea of reverse movements along the entire onshore portion of the fault [28] or only along its western segment [27] has not been proved by factual evidence and followed only from general reasoning, e.g., from strike of the fault at an angle to the submarine right-lateral Bering Fault (Fig. 2).

On land, the fault is distinctly subdivided into the western and eastern parts approximately equal in length and with a two-kilometer gap between them. The eastern part of the near-latitudinal segment of the Kamchatsky Mys Range is the southern side of both parts of the fault (Fig. 3). The northern sides differ in geological structure. The northern side of western part is a depression filled with upper Pliocene–Eopleistocene sediments of the Ol'khovaya Formation [2, 4]. The depression opens into the central basin of the peninsula occupied by lakes Nerpich'e and Kultuchnoe. The eastern part of the fault bounds in the south a wide and relatively short basin with the Second Pereval'naya River valley between the nearly meridional

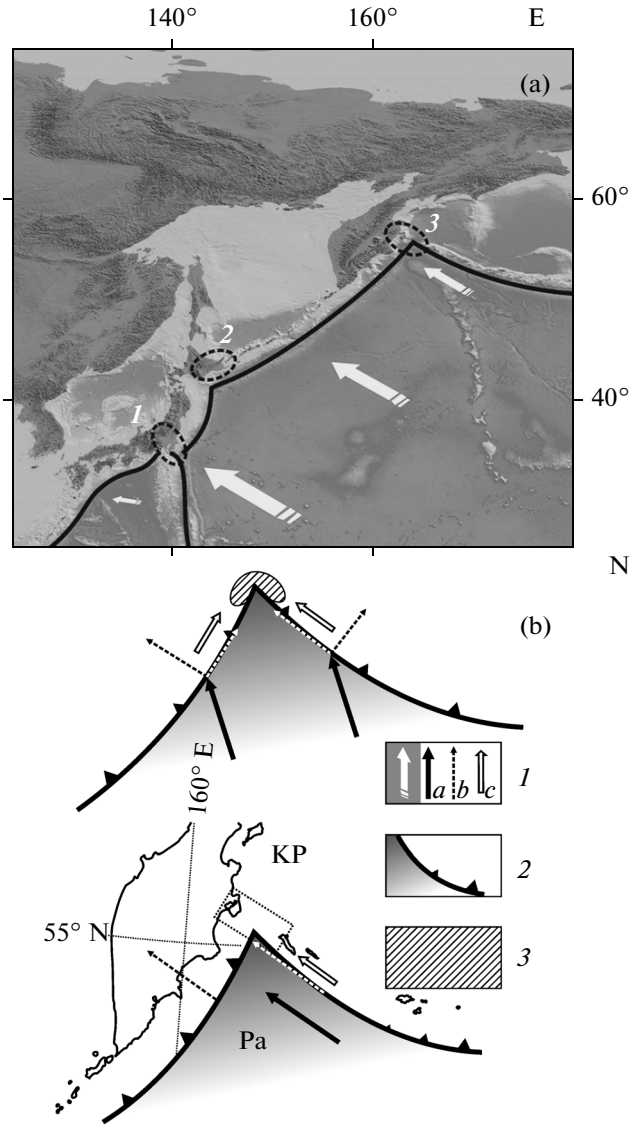

Fig. 1. (a) Collisional interaction of island arcs in the northwestern Pacific: *1*, Izu–Bonin and Japan; *2*, Japan and Kurile–Kamchatka; *3*, Kurile–Kamchatka and Aleutian; bathymetry and topography, after SRTM30_PLUS [17]; (b) conceptual scheme of tangential and normal components of oceanic plate motion relative to island arcs (above) and their relationships in the junction of Kamchatka and Aleutian island arcs (below). (*Ia*) Direction of the Pacific Plate motion, (*Ib*) orthogonal and tangential components of plate motion relative to island arcs, (*Ic*) direction of motion of part of island arc toward collisional zone; (*2*) subduction zone; size of triangular ticks shows increase (decrease) of underthrusting (normal) component; (*3*) collisional domain. Rectangle (dotted line) in panel (b) is position of Fig. 2; KP, Kamchatksky Peninsula; Pa, Pacific Plate.

(Mount Komandnaya) and east-striking (Mount Afrika) segments of the Kamchatsky Mys Range. Several intrabasinal uplifts are composed of Cretaceous rocks of the Smagin and Pikezh formations [4]. Their flat tops, apparently representing fragments of one (two?) Pleistocene marine terraces, gradually get lower

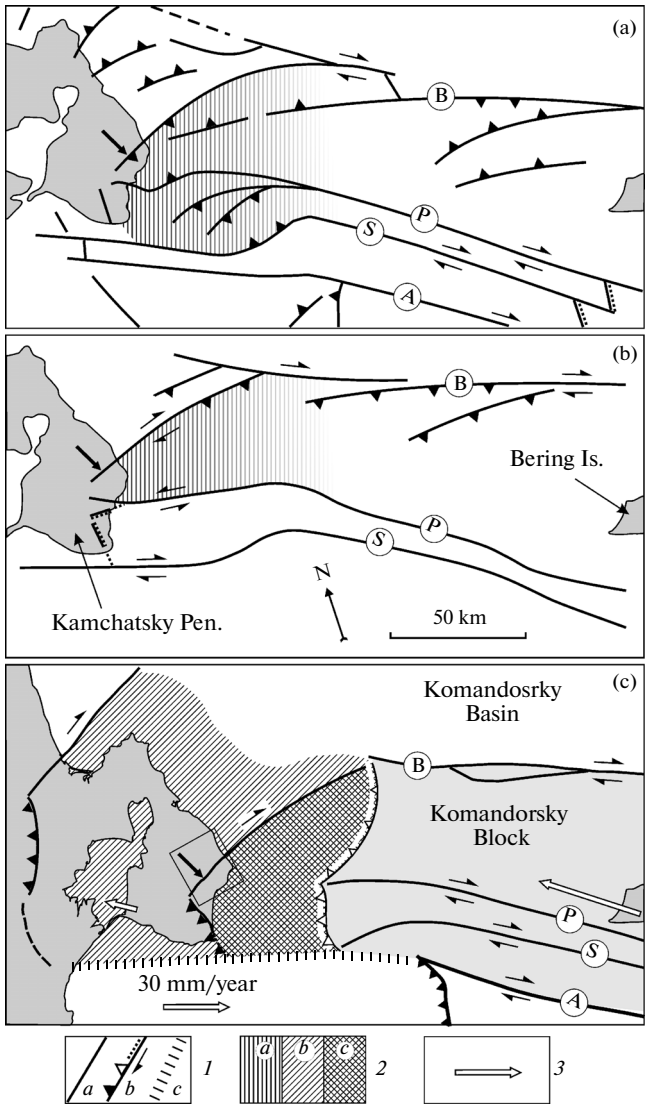

Fig. 2. Models of collisional interaction between Aleutian and Kamchatka island arcs, modified (a) after [28], (b) after [1], (c) after [8]. (*1a*) Major active faults; (*1b*) sense of movements along reverse and thrust (triangles), strike-slip (arrows), and normal (dots) faults; (*1c*) subducted edge of the Pacific Plate; (*2a*) frontal part of Komandorsky Block in panels (a) and (b); (*2b*) block of the western (major) and (*2c*) southeastern parts of Kamchatsky Peninsula in panel (c); (*3*) vectors of GPS station migration in panel (c), after [20]: western arrow is station in Krutoberegovo Settlement, eastern arrow is station in Bering Settlement. Submarine faults of Komandorsky segment of Aleutian arc (letters in circles): B, Bering; P, Pikezh; S, Steller; A, Aleutian (axis of the Aleutian trench); shown in panel (c) after [13]. Black arrows in panels (a), (b), and (c) point to Second Pereval'naya Fault. Rectangle in panel (c) contours Fig. 3.

seaward at a general slope of ~3° (Fig. 3, inset (b)). The northern wall of the basin is probably also bounded by a fault. A scarp about 100 m high occurs near the shore on the trend of the northern limitation of the basin. The same Late Pleistocene terrace is localized to the north and south of this scarp. This terrace formed approximately 120000 years ago during the marine isotopic stage of the MIS 5e [40, 41] (Fig. 3). No indications of displacements along this fault in the Holocene have been documented.

METHODS

Observation and Interpretation of Faulted Sediments

The technique applied to study sedimentary rocks displaced along faults is now standard and does not require special description. In particular, it was considered in detail in *Paleoseismology* [38, 39]. In general, this technique uses traditional methods of structural geology and analysis of facies and thickness aimed at recognition and dating one or several ground surfaces that existed at the moments of the faulting events, in order to ascertain sense and amplitude of individual offsets, their age, and average recurrence intervals. These movements rupture ground surface and initiate a number of exogenic processes, without knowledge and consideration of which reliable interpretation of the faulted section is impossible.

Determination of Kinematic Parameters of a Fault from Deformed Landforms

Determination of the sense and rate of movements along a fault from offsets of erosion network elements is an ordinary and longstanding technique. The study of wave-built marine terraces for this purpose is a complicated task, which requires identification and division of the contributions from eustatic fluctuations and tectonic movements proper to their formation.

The wave-built marine terraces form by attachment of beach ridges different in age to one another. The attachment is prolonged in time, so that to speak of the age of a wave-built marine terrace, it is reasonable to indicate the time interval when the oldest and the youngest beach ridges making up the given terrace formed. Morphological attributes, in particular, scarps and shoreline angles dividing terrace levels, are commonly used for recognition of marine terrace levels, although these levels can be so close in age that they must be combined into a single terrace. The height and shape of a beach ridge depend on the wave energy and sediment supply. Therefore, a beach ridge that formed during a period between movements along a fault crosscutting wave-built marine terraces has approximately the same height and morphology on both sides of the fault. When a terrace is displaced along a fault, part of the beach ridge in the fault side uplifted and shifted away from the sea may leave the zone of active beach, whereas another part located in the fault side downthrown and shifted seaward may be partly or completely eroded. Thus, having dated beach ridges or shoreline angles of different terrace levels and revealed coeval ones on opposite sides of the fault, we can reconstruct the sense and amplitude of displacement

along the fault and estimate the time interval when this displacement took place.

To determine the approximate age of each terrace level, the tephrochronological method has been used [19, 36]. Thus, the volcanic tephra interbeds at the top of marine sand in excavations near the shoreline angles of terraces were identified. This technique was described by Pinegina et al. [11, 42]. Tephra layers are clearly seen as bright interbeds against the background of relatively dark soil and marine sand.

The average rates of net vertical shore movements (V, mm/yr) and for the time intervals between the formation of separate terrace levels were estimated from the relationship $V = (H - H_0)/t$, where H is the height of shoreline angle above sea level at the moment of measurement; H_0 is the height of a certain zeroth elevation mark above sea level at the moment of measurement; t is the difference in age between terrace levels H and H_0 [11, 42]. The height of shoreline angles is determined by measuring of topographic profiles with measurement points at each bend of the topography, including those in the shoreline angles of terrace levels differing in height. As was established by the earlier study [11], the line of maximum storm inundation rather than the mean sea level should be used as the zeroth mark in comparing terrace heights, because the height of the terrace depends on the energy of waves, which varies at shores with different expositions. The tectonic constituent of the difference in terrace heights is determined by subtracting the exogenic constituent from the total height difference. It is known that the height of the line of maximum storm inundation along the shore of the Kamchatsky Peninsula varies from 3.5 to 7.5 m [11, 42], and that the line of the maximum storm inundation is marked by transition from pioneer plants to first dense vegetation. Comparison of relative heights of shoreline angles along one profile is based on the assumption that the wave energy remained constant during the formation of terraces at a given point of the shore and that storm activity did not change significantly during the past ~2000 yr. To estimate the absolute rate of vertical movements, a correction for along-shore variation of storm activity is necessary.

Taking into account that the deformation of young landforms as a result of one or several offsets along the fault is small and cannot be revealed in topographic maps on scales of 1 : 50000 and 1 : 100000, the portion of the Second Pereval'naya Fault was covered by a topographic survey using a Trimble-3m electron laser tacheometer. The horizontal step of the survey did not exceed 2 m, on average. The detailed digital topography model prepared as a result of surveying was used to further measure the horizontal and vertical displacements along the fault.

Dating of Sediments

Holocene loose sediments in Kamchatka are distinguished by the occurrence of volcanic ash (tephra) interbeds. This feature made it possible to use the tephrochronological method to estimate the rate of movements along the fault [36]. We studied tephra layers exposed in excavations to date marine terraces and displacements along the faults. The applied technique was described in [11, 35, 42]. To do this we correlated tephra layers with those previously studied and dated in the area [9, 11] to estimate their age and volcanic sources. Some samples of tephra from the base of excavations were also used for microprobe analysis of volcanic glass carried out on a JEOL JXA 8200 microprobe (GEOMAR, Kiel, Germany).

To date landforms and sediments in the studied area, the following tephra units were used: SH_{1964} (1964 A.D., Shiveluch volcano), SH_{1450} (~1350 yrs BP, Shiveluch volcano), KS_1 (~1650 yrs BP, Ksudach volcano); PL2 (~ 10200 yrs BP, Ploskie Sopki [Flat Hills]) [10, 18, 43]. The age of tephra related to the historical eruption of Shiveluch volcano in 1964 is given as a calendar date, whereas the ages of other tephra interbeds determined by radiocarbon method are in years before 1950 (calibrated age BP).

SENSE AND AVERAGE RATE OF MOVEMENTS ALONG THE SECOND PEREVAL'NAYA FAULT

Eastern Part of the Fault

At the shore, the Second Pereval'naya Fault crosscuts a series of Pleistocene wave-cut and Holocene wave-built marine terraces and approaches the shoreline at almost right angle. The Holocene marine terraces are attached to the cliff of the youngest of Pleistocene terraces, presumably 120000 years in age [40, 41] (Fig. 3).

A trench has been excavated few tens of meters from the cliff edge at the base of the fault scarp on the Pleistocene terrace. The aim of trenching primarily was to corroborate real existence of that fault.

Age and recurrence interval of movements along the fault from the data on deformed section. The section exposed in the trench comprises poorly lithified and strongly altered agglomerate in silty matrix and soil–pyroclastic cover with KS_1, SH_{1450}, and SH_{1964} tephras (Fig. 4). The section is broken by two fault planes steeply dipping southward. With the downthrown northern side, this implies that vertical movements are reverse. The small step at the fault scarp surface and details of the deformed section show that approximately 3 m to the south from the southern margin of trench there may be one more fault plane (Fig. 4a).

The undisturbed part of the section is observed in the northernmost part of the trench, i.e., in the downthrown side of fault and composed of the base of soil–pyroclastic cover (1), soil layer (2) with KS_1 (3)

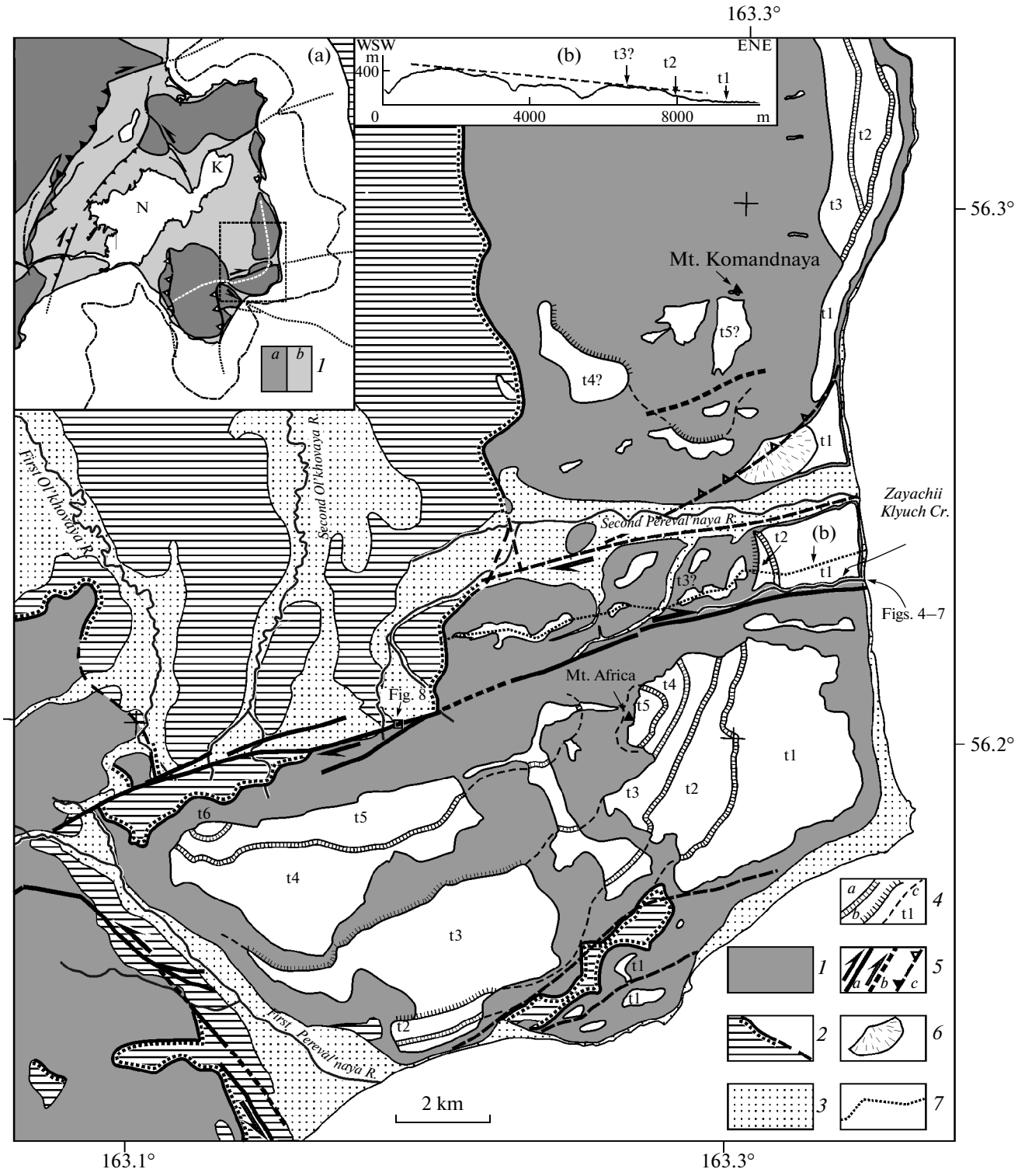
163.3°
56.3°
56.2°
163.1°
163.3°
(a)
(b)
WSW
ENE
m
400
0
4000
8000
m
t3?
t2
t1
K
N
a
b
1
Mt. Komandnaya
t5?
t4?
t2
t3
t1
First Olkhovaya R.
Second Olkhovaya R.
Second Pereval'naya R.
Zayachii Klyuch Cr.
Figs. 4–7
Fig. 8
Mt. Africa
t4
t5
t6
First Pereval'naya R.
2 km
2
3
4
5
6
7

Fig. 3. Active faults in southeastern Kamchatsky Peninsula (see inset (a) and Fig. 1c for location). (*1*) Pre-Pliocene rocks, after [4]; (*2*) Pliocene–Eopleistocene Ol'khovaya Formation (hatched), in the right side of the First Pereval'naya River valley is combined with Eoleistocene–lower Neopleistocene marine sediments [4]; dotted line is unconformable boundary; dashed line denotes inferred position beneath overlying sediments; (*3*) late Pleistocene–Holocene sediments and landforms; (*4*) Pleistocene marine terraces (numeration (t) from younger to older) and dividing scarps: (*a*) with retained shoreline angle and crest, (*b*) with eroded crest, (c) approximate position of shoreline angle in areas, where terraces have been eroded; (*5*) faults: (*a*) active, (*b*) probable extensions of active faults and presumably active faults, (*c*) Quaternary, currently inactive; filled symbols when sense of movement is known (arrows and triangles denote strike-slip and reverse faults, respectively); open symbols indicate inferred kinematics; (*6*) large fans and landslides; (*7*) line of topographic profile shown in inset (b). Inset (a): active faults in Kamchatsky Peninsula, modified after [8]. (*1*) Relative (*a*) uplifts and (*b*) depressions; black dotted line is shelf edge; white dotted line is drainage divide of Kamchatsky Mys Range; rectangle is location of Fig. 3; N, Nerpich'e Lake; K, Kultuchnoe Lake. Inset (b), topographic profile (dotted line in figure).

and SH_{1450} (4) tephra followed upsection by mixed soil and slope-derived sediments (8), overlying SH_{1964} tephra (9), and a layer of currently forming soil with falling plant detritus (10) (Fig. 4b). The structure of section changes when approaching the fault. A wedge of coarse sediments (5) appears in the soil profile between KS_1 and SH_{1450} tephras; soil layer (2) doubles and is overlapped by coarse sediments (6) and (7); the slope-derived sediment and soil unit (8) abruptly increases in thickness and bear indications of downslope movement. In the southern wall, the KS_1 and SH_{1450} tephra layers are disintegrated, and wedge of slope-derived sediments (5) between them rapidly increases southward.

Lenses and wedges (5–7) composed of coarse basal material (1) indicate repeated movements along the fault. Wedge (5) between the KS_1 and SH_{1450} tephra, whose thickness increases southward, apparently represents the distal portion of colluvial sediments, the appearance of which could have been related to a movement along the fault plane not exposed by the trench. The wedge overlies the lower part of the soil layer (2a) that had accumulated by the moment of movement. The displacement of all units of the section, including wedge (5) up to the upper part of soil layer (2b), is a result of younger movement along the fault plane exposed at the trench wall. Its relative age is determined by the age of the roof of soil layer (2) overlain by lenses (6) and (7). The tops of layers (2a) and (2b) overlain by colluvium are the paleosurfaces that existed at the moment of movements (event horizons) (Fig. 4b).

The absolute age of both movements can be estimated in the following way.

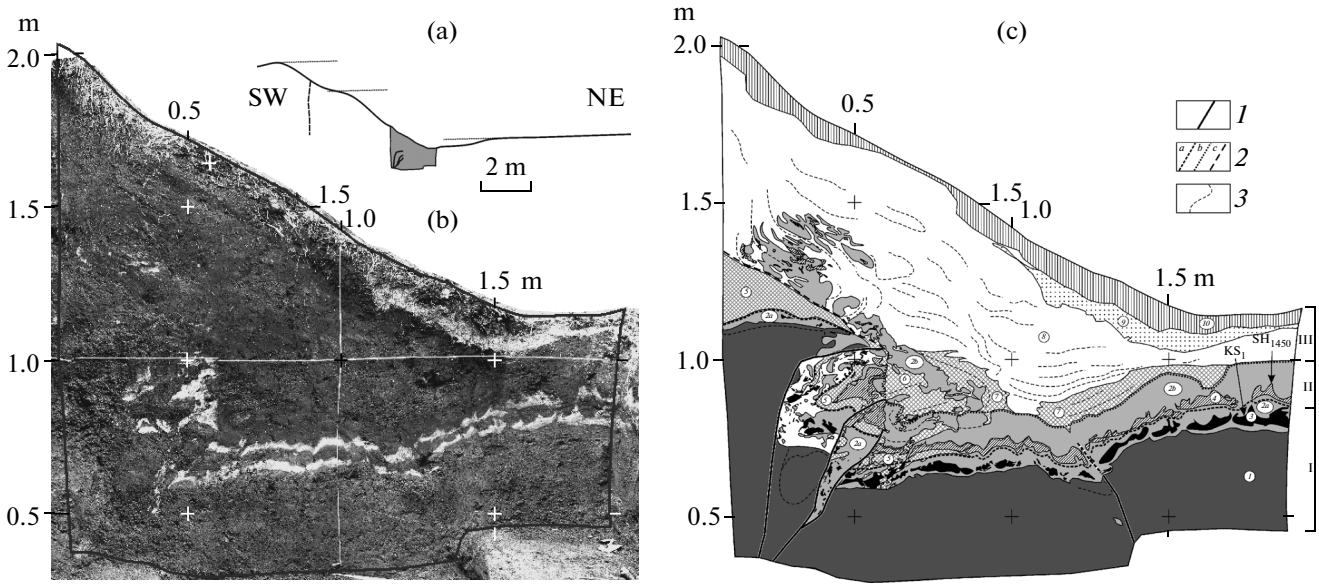

Fig. 4. Section of soil–pyroclastic cover at northwestern wall of trench across Second Pereval'naya Fault: (a) topographic profile across the lower part of fault scarp and location of trench; (b) photograph of trench wall (black line along perimeter is contour of sketch in panel (c)); (c) sketch of deformed section with elements of interpretation; (*1*) fault plane; (*2*) paleosurfaces displaced during (*a*) the first and (*b*) second movements; (*c*) erosion surface; (*3*) visible bedding surfaces. Numerals in circles and ovals are units; Roman numerals denote sediments deposited before first (I), second (II), and after second (III) movements. Distances in meters along perimeter of trench wall (panel (b)) and in sketch (panel (c)) are given relative to conventional zero below southwestern corner of trench. Photograph in panel (b) and sketch in panel (c) are presented on the same scale.

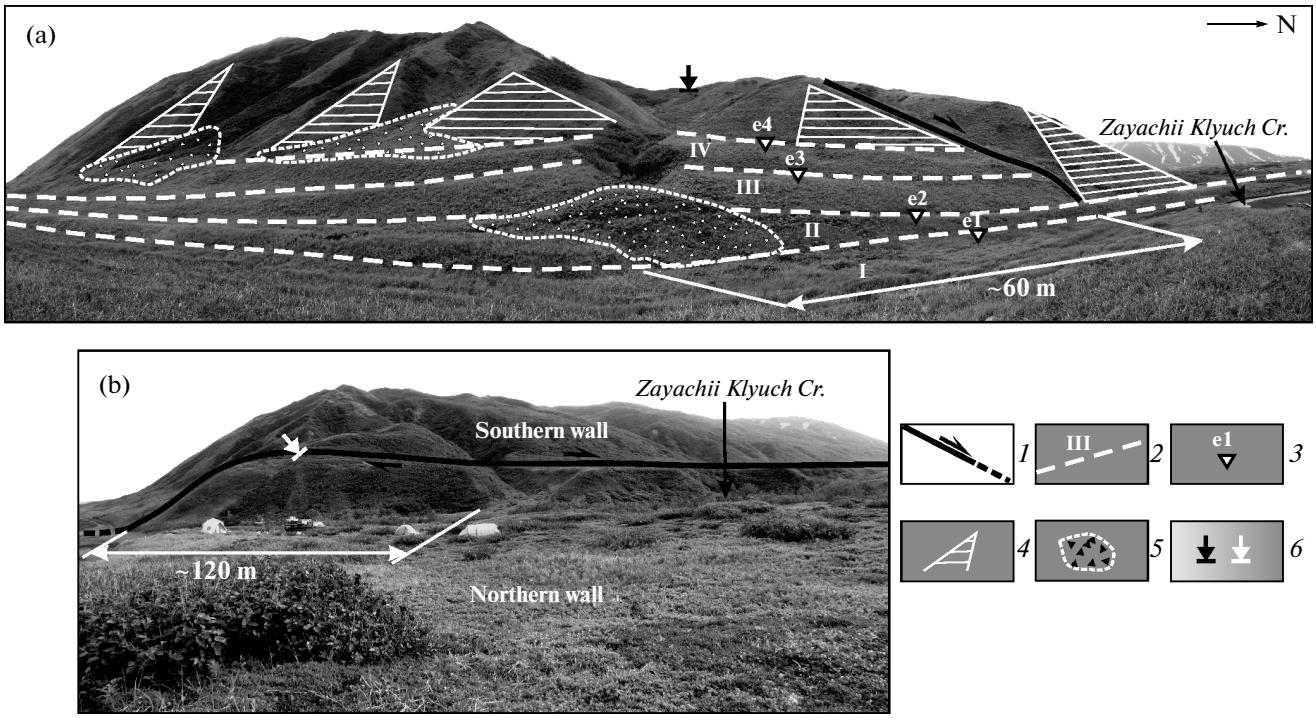

Fig. 5. Panoramic view of the Second Pereval'naya Fault by the shore of the Kamchatsky Strait: (a) view from east (shore) and (b) from north. (*1*) Fault; (*2*) shoreline angle of terrace level and its number on Holocene wave-built terrace; (3) excavation and its number; (*4*) relict paleocliff; (*5*) fan; (*6*) trench across fault-line scarp on terrace MIS 5e (see Fig. 3).

The thickness of soil layer between KS_1 (~1650 yrs BP) and SH_{1450} (1350 yrs BP) tephras is ~3.5 cm (average of five measurements); the time interval of its deposition (difference between calibrated ages of the divided tephras) is approximately 300 years. This implies that a mean rate of soil growth is ~0.1 mm/yr. At such a rate, a part of the soil profile (2b) approximately 8 cm in thickness (average of four measurements) overlying SH_{1450} tephra could have developed approximately over 800 years. This implies that the age of paleosurface at that moment when it had been overlain by colluvial material of lenses 6 and 7 and the corresponding age of the most recent movement is ~550 years. The vertical separation on the fault (the difference between the base of the soil–pyroclastic cover in the southernmost and northernmost parts of the trench) was 0.30–0.35 m.

The age of the penultimate faulting movement can be approximately estimated in the same way.

Accumulation of the soil layer approximately 3 cm in thickness (average of five measurements) between KS_1 tephra and colluvial wedge (5) took about 300 years. This implies that the Earth's surface upon which colluvial wedge (5) rests, and movement itself, is about 1350 (1650–300) years old. Deposition of alternating soil, slope-derived, and mixed sediments of unit (8) variable in thickness and extent beneath the lower part of the faultline scarp after 550 years ago could have been related to the movements along the fault plane uncovered by trenching. The number of movements responsible for the formation of unit (8) cannot be exactly determined. If the layers of coarse slope-derived sediments between soil layers are interpreted as evidence for movement along the fault plane beyond the trench, then at least, one to two additional movements could be added.

As follows from the aforesaid, the average time interval of recurrent movements along the fault is approximately 800 years.

Sense, Amplitude, and Rate of Movement along the Fault from Study of Holocene Wave-Built Marine Terraces

Geomorphic characterization of the terrace. The shore on opposite sides of the fault looks differently (Fig. 5). Four Holocene terrace levels and recent active beach are distinguished on the southern fault side. The highest and oldest terrace is attached to the now inactive cliff, which was active and scoured between reaching a maximal sea level in Holocene about 6000 years ago and onset of the formation of the wave-built marine terrace. The width of separate terrace levels on southern side of the fault reaches 20–35 m; the total terrace width together with beach is about 150 m.

Only two lower terrace levels and active beach extend to the northern side from the southern side remaining undisturbed by the fault.

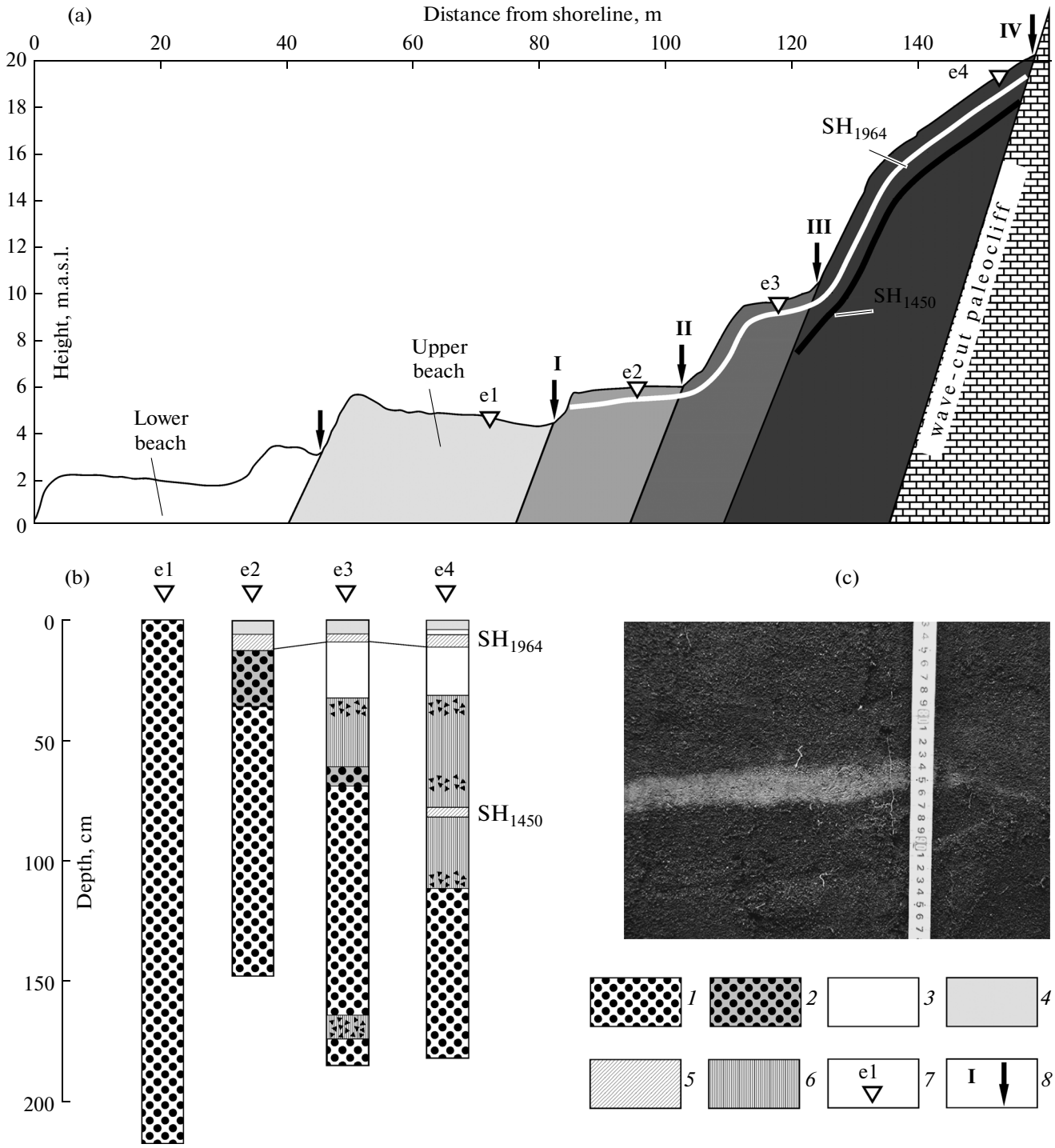

Fig. 6. (a) Topographic profile and (b) geological section of the marine terrace in the southern side of Second Pereval'naya Fault. (*1*) Clean marine sand; (*2*) marine sand with humified sandy loam; (*3*) humified sandy loam; (*4*) turf; (*5*) tephra; (*6*) humified soil and slope-derived sediments; (*7*) excavation and its number; (8) shoreline angle and ordinal number of terrace level; SH_{1964} and SH_{1450}, tephra from Shiveluch volcano. Levels I and II extend continuously to northern side of fault; levels III and IV are retained only in the southern side. Photograph (c) is fragment of wall in excavation 4 with SH_{1450} tephra.

The sections in excavations at each terrace level along the profile reveal the following features (Fig. 6). At level I located above the still not overgrown part of active beach, no volcanic ash has been revealed. Level I itself has not still gone out of zone of storm inundation, and thus represents the upper active beach. Its section is composed of clean, humus-free marine storm sand with graded bedding.

No volcanic ash older than SH_{1964} has been identified at level II. The upper 30-cm portion of the section

Table 1. Height, age, and rate of vertical motions for wave-built marine terrace at intersection with Second Pereval'naya Fault

Terrace level	I	II	III	IV
Level height relative to line of maximal storm inundation	0	1.5	5.5	14.5**
Age of shoreline angle, years (calibrated age)	modern	~200	<1400	~1650
Mean rate of vertical tectonic motions, mm/yr		7.5	*	8.3

* Rate of vertical motion for level III was not determined because of inaccurate estimation of its age.

** Without 1 m taken as total thickness of soil and colluvial material.

consists of marine sand colored with humus. The experience of our study shows that humus forms at the shore beyond the zone of storm inundation. Therefore, it is assumed that terrace level II became a relict (inactive) part of the wave-built terrace no earlier than a few hundreds of years ago.

The lower part of the soil–pyroclastic cover overlapping terrace level III lacks volcanic ash older than SH_{1964}. The soil profile here contains a layer of humified sandy loam as thick as 60 cm and an underlying 10–15-cm bed of humified marine sand. With allowance for the structure of this soil profile and its comparison with the adjacent profiles, it is assumed that level III could have become a relict site of the terrace probably soon after fall of SH_{1450} tephra.

The layer of humified soil at terrace level IV is 115 cm in thickness. At a depth of 80 cm, the soil contains SH_{1450} tephra, whereas somewhat older KS_1 tephra dated 1650 yrs BP is absent. Thus, it is as though level IV is younger than KS_1 tephra, but it is close to the latter in age, because a break between the fall of SH_{1450} and KS_1 tephras was only 300 years.

The highest terrace level level adjoining the cliff is inclined seaward much more steeply than the younger levels (Fig. 6). This could have been caused by an initially steeper slope of the active beach during formation of this area or by accumulation of the material derived from the surface of wave-cut cliff, at the foot of which this terrace is located. The cliff is not active currently, however, the soil–pyroclastic cover overlying the terrace contains three interbeds of slope-derived sediments each 5–10 cm thick. Thus, material was probably supplied to the terrace from time to time as a result of the impact of tsunami waves on the shore or due to movements along the fault.

Rates of vertical movements. In the measured topographical profile (Fig. 6), the width of lower active beach both to north and south of the fault crosscutting the terrace is ~45 m. The height of the scarp between the lower and upper active beaches, i.e., the height of the shoreline angle of the lower beach, is 3 m above the mean sea level. The scarp is not the result of tectonic uplift; it formed under the impact of storm waves, and its position changes depending on season and from year to year. The boundary line of first dense vegetation spatially coincides with the shoreline angle of level I (upper active beach) and occurs ~1.5 m above the shoreline angle of the lower beach, i.e., at a height of 4.5 m. The position of this line relative to the mean sea level indicates the height above which the marine terrace does not experience the influence of storms except for tsunamis and is retained as a landform for a long time; i.e., it becomes a relict [11].

The relative heights of different terrace levels and rates of vertical movements calculated from these data are shown in Table 1.

As mentioned above, only two lowermost terrace levels I and II are continuously traced from one side of the fault to another. These levels have not been displaced either laterally or vertically. This indicates that the most recent movement along the Second Pereval'naya Fault took place before formation of level II but after formation of levels III and IV, i.e., in the time interval of 1400 to 200–300 yrs BP (calibrated age). In general, this corresponds to the age of the most recent movement (~550 yrs BP, calibrated age), which has been established by studying the deformed section opened in the trench (see above).

The undeformed levels I and II on both fault sides indicate that the formation of marine terraces themselves is independent of vertical movements along the fault. In the time interval between movements, the shore undergoes the common tectonic uplift, when the shore segments on opposite sides of fault emerge simultaneously with the same rate. This suggestion is consistent with approximately equal rates of uplifting for deformed (IV) and undeformed (II) levels (Table 1). At the same time, the movements along the fault resulted in uplifting of levels III and IV south of the fault and erosion of them north of the fault. In other words, disappearance of the upper levels in the northern fault side is caused by movements along the fault. To be eroded, levels III and IV must have subsided below the line of maximum storm inundation, i.e., approximately below 4.5 m above the mean sea level. Thus, the total vertical separation must be a minimum of no less than 14.5 m for level IV and no less than 5.5 m for level III. It is evident that such throw amplitudes are cumulative, and several movements along the Second Pereval'naya Fault took place over the last ~1700 years after the fall of KS_1 tephra (see description of trench above).

The rates of vertical movements of shore far from the fault were previously calculated also for the last

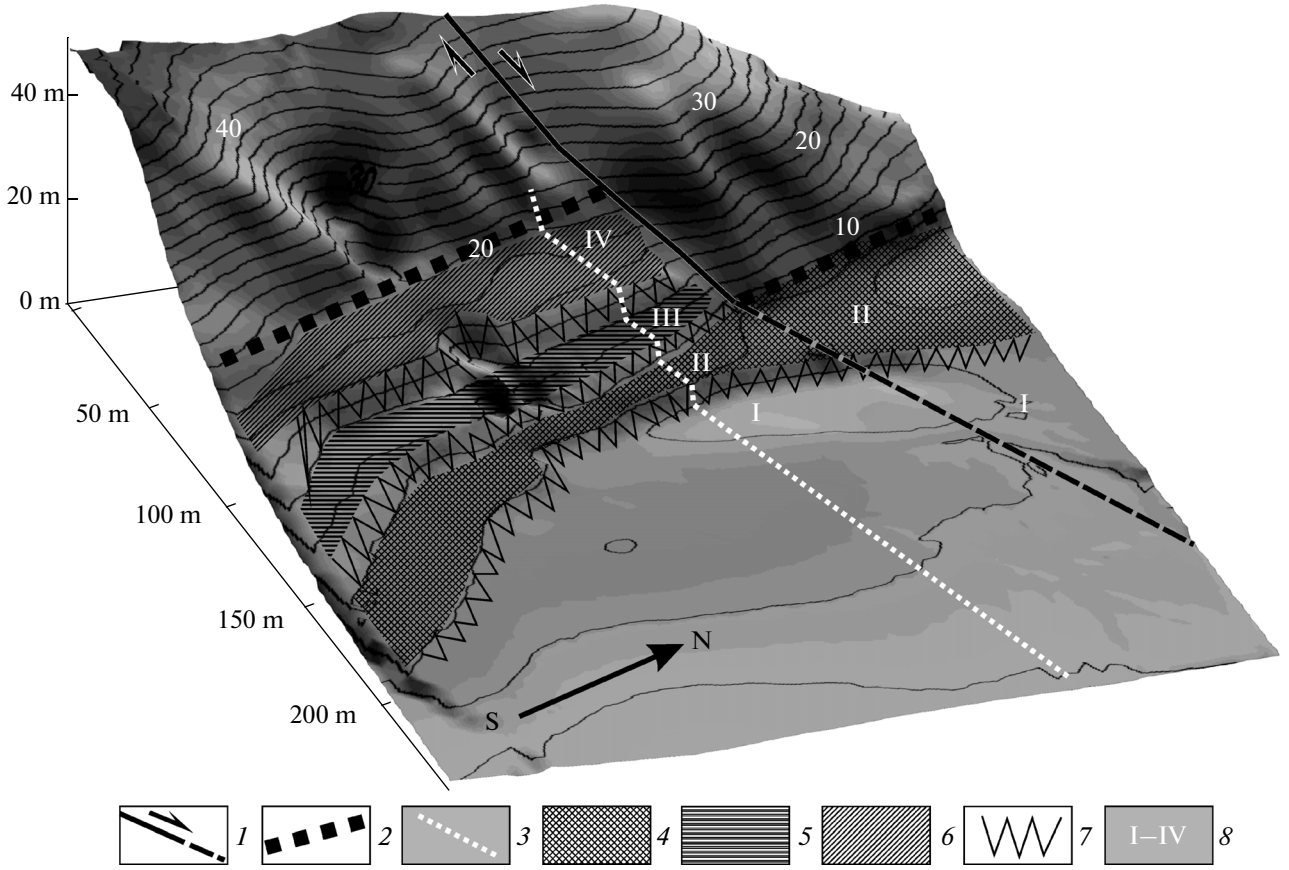

Fig. 7. 3D model of topography of wave-built marine terrace cut by the Second Pereval'naya Fault. (*1*) Fault line along which landforms and sediments have been deformed; dashed line is segment of fault where young marine terrace remains undeformed; (*2*) abrasion cliff displaced along fault 30–32 m; (*3*) topographic profile; (*4*) terrace level II undeformed by fault; (*5, 6*) terrace levels III and IV retained only in southern uplifted side of fault; (*7*) scarps separating terrace levels; (*8*) terrace level number. Contour lines are spaced at 2 m.

1650 years [11, 42]. The mean rates of vertical movements of the shore to the south of fault is ~7 mm/yr. To the north of the fault, the shore either remains stable or submerges. The obtained estimates of the vertical movement rate along the fault are approximately equal to the difference in rates of movements of shore to the north and south of the fault.

Rates of horizontal movements. The paleocliff, against which the late Holocene wave-built marine terraces lean, is displaced 30–32 m right-laterally. This value, obtained by measurement based on the digital topography model, cannot be attributed to the time interval of 6000 years that elapsed from the time when the cliff became active at the maximum sea level

Table 2. Chemical composition (wt %) of volcanic glass from tephra interlayer at base of soil–pyroclastic cover overlying displaced terrace of creek

Sample	SiO_2	TiO_2	Al_2O_3	FeO	MnO	MgO	CaO	Na_2O	K_2O	P_2O_5	SO_3	Cl	Total
263-4	58.84	1.43	16.13	7.53	0.17	2.79	6.13	3.89	2.43	0.59	0.04	0.04	100.00
	59.07	1.44	16.00	7.38	0.07	2.86	6.07	3.93	2.46	0.69	0.01	0.03	100.00
	58.80	1.40	15.93	7.67	0.14	2.81	5.98	4.13	2.44	0.62	0.03	0.04	100.00
	58.76	1.42	16.04	7.85	0.09	2.84	6.08	3.82	2.39	0.63	0.06	0.03	100.00
	58.58	1.39	16.09	7.94	0.13	2.90	6.01	3.76	2.44	0.70	0.02	0.04	100.00
	59.08	1.39	15.81	7.67	0.19	2.76	5.93	3.91	2.46	0.69	0.06	0.04	100.00

Analyses carried out on JEOL JXA 8200 microprobe, analyst M.V. Portnyagin (GEOMAR, Kiel, Germany). Analyses normalized to 100 wt % volatile free.

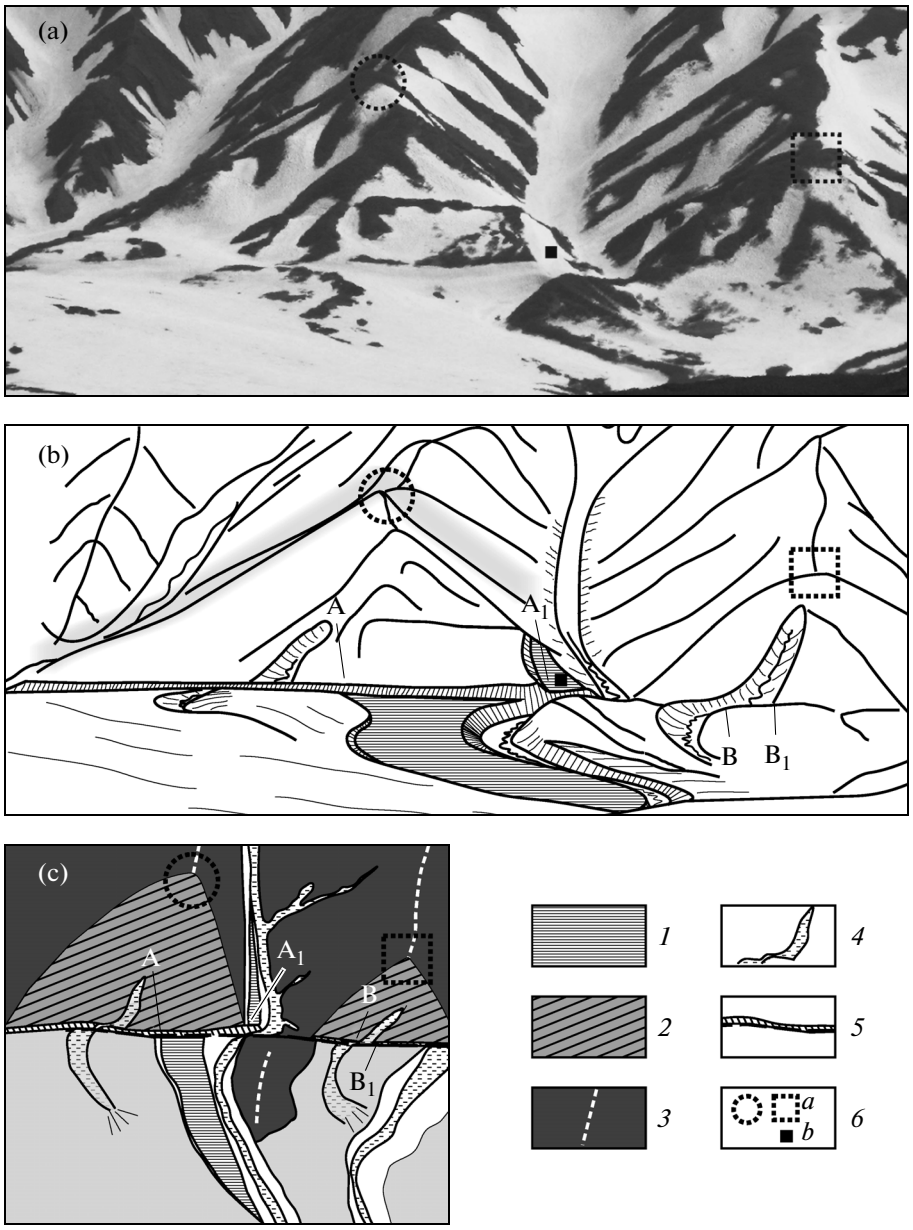

Fig. 8. Offsets of landforms at eastern end of western segment of Second Perevel'naya Fault: (a) photograph (view to the south), (b) sketch after this photograph, (c) plan view. (*1*) Displaced terrace; (*2*) facets above young fault scarp; (*3*) drainage divide; (*4*) active channel; (*5*) scarp along fault line; (*6*) landforms (*a*) and excavations (*b*) repeating in panels (a), (b), and (c). Distances $A–A_1$ and $B–B_1$ correspond to horizontal offsets (see text for explanation).

in the Holocene. Before attachment of late Holocene terrace level IV, the cliff underwent intense scouring facilitated by the low mechanical strength of rocks of the Cretaceous Smagin Formation (fractured basalt, dolerite, tuff, tuffaceous siltstone, chert, limestone) [3]. The abrasion rate even for rocks most resistant to disintegration, to which the Smagin Formation cannot be referred, is about 1 cm/yr [5]. For unstable rocks, this rate can reach tens of meters per year, and under specific conditions of the studied site, could have exceeded the rate of movement along the fault. Thus, to estimate the slip rate, we used the age when the cliff terminated its activity during the onset of aggradation of terrace level IV about 2000 years ago rather than the age of the initial cliff formation.

The distance along the fault line between the intersection with shoreline angle of the displaced terrace and the foot of the paleocliff on the opposite fault side, which coincides in plan view with the shoreline angle of undeformed terrace level II, was taken as the horizontal offset (Fig. 7). The results of topographic survey have shown that the shoreline angles of levels III and IV are offset laterally along the fault 5–6 and 30–32 m,

respectively. Both offset values should be regarded as minimal.

As follows from the available data, a minimal mean value of the rate of right-lateral movements along the Second Pereval'naya Fault over ~1700 years is 18–19 mm/yr.

Western Part of the Fault

The largest of the revealed horizontal offsets of landforms along the western fault segment were observed at its eastern end, at the observation point with coordinates 56.2012° N and 163.1876° E (Fig. 8; see Fig. 3 for location). The measurement of the right-lateral offset of the right side of the stream running down from the Kamchatsky Mys Range into the basin of the Second Pereval'naya River, using aerial photograph linked to the geographic coordinate system, yielded approximately 150 m. This value differs by almost one-fourth toward the larger side from the previous estimate based on visual evaluation [6, 34)]; it is accepted as more accurate.

A pit was dug on the southern side of the fault at the surface of stream terrace, the shoreline angle of which was displaced for the aforementioned distance. Several tephra interbeds were found in the opened soil–pyroclastic cover in excavation overlapping the creek's alluvium. The composition of volcanic glass from the lowermost ash interbed was identical to the composition of glass from PL2 tephra related to the volcanic center of Ploskie Sopki and dated at a calibrated age of ~10 200 years (Table 2; Fig. 9) [43]. The axis of ash fall extended through the studied area, and this corroborates the validity of the correlation. Thus, the terrace most likely formed in the early Holocene, and the mean rate of Holocene offsets was 14–15 mm/yr. The vertical separation of this fault segment was incommensurably smaller in comparison with the horizontal offset. The fluvioglacial (?) surface, the terrace deformed by the fault incised in, was displaced approximately 5 m vertically. Thus, the minimal ratio of the horizontal to vertical components of movement is 30.

DISCUSSION

The study of the fault-deformed sediments has shown that two movement events, which took place over the last 1700 years, were separated by a time interval estimated at ~800 years. This conclusion is inconsistent with the amplitudes of vertical and horizontal displacements over the same time, estimated from studying the deformed marine terrace. Attribution of the cumulative horizontal offset (30–32 m) to the two events yields a one-event offset of about 15–16 m; this value cannot be taken as a real without additional substantiation. Individual vertical offset is also far from reality if the 14.5 m of relative subsidence of the northern side of the fault is attributed to the two events. The available data provide no insights into this inconsis-

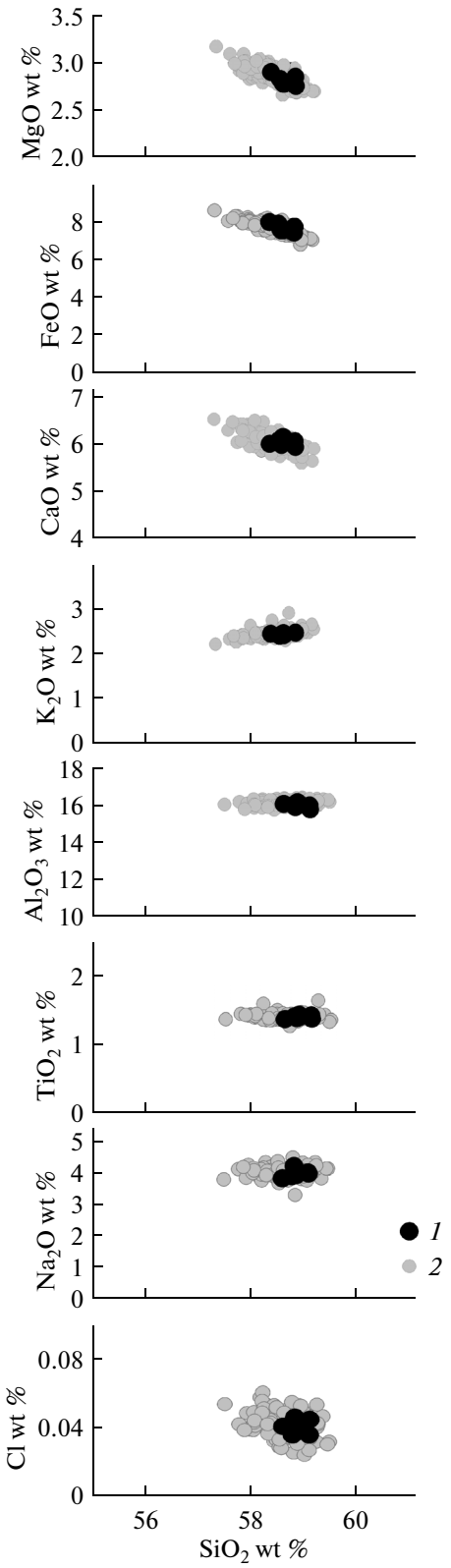

Fig. 9. Contents of major and some minor elements in glass from (*1*) tephra at base of soil–pyroclastic cover on terrace displaced by fault and (*2*) from PL2 tephra, after [43].

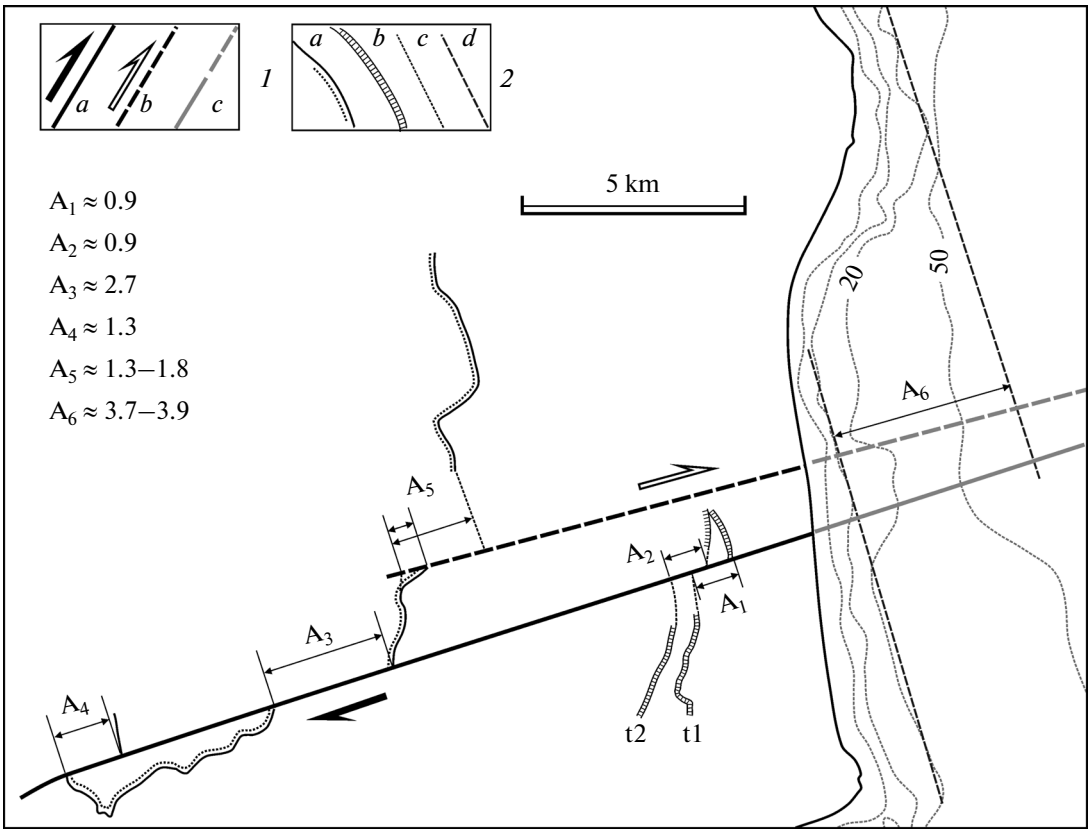

Fig. 10. Right-lateral offset of pre-Holocene rocks and landforms along the Second Pereval'naya Fault. (*1*) Faults: (*a*) active, (*b*) inactive, and (*c*) their submarine extensions (schematized); (*2*) displaced geological and geomorphic elements: (*a*) boundary of Ol'khovaya Formation (dotted line is unconformable contact with older rocks), (*b*) shoreline angle of marine terrace; (*c*) inferred position of displaced elements overlapped by loose Quaternary sediments or subsequently eroded; (*d*) base of submarine slope (approximation of 20 m isobath, after [4]). A_1–A_6 are amplitudes of horizontal offsets, km.

tency. We only can assume that the fault splits into more than two planes near the Earth's surface, which did left no traces in the section exposed in the trench.

The mean slip rate along the eastern segment of the fault over the last 1600–1700 years is 18–19 mm/yr. The rate was probably even higher, because the calculation does not take into account the time that elapsed after the most recent movement. The mean rate of horizontal offset along the central segment of the fault in the Holocene calculated over the first 8000 years without cumulative offset (~30 m) over the last 1700 years is somewhat lower (13.5 mm/yr). It should be noted that the estimated mean rates are sufficiently rigorous. Their comparison indicates that the rate of horizontal movements along the Second Pereval'naya Fault in the Holocene increased with time. Judging by the reverse sense of vertical component of movements, they developed under transpressional conditions.

Comparison of slip rates in the Holocene with those that followed from older offsets also demonstrates the time-dependent acceleration of horizontal movements along the fault. For example, the right-lateral offset of the shoreline angle of the late Pleistocene terrace MIS 5e (~120000 years) along the eastern segment of the fault is ~900 m (Fig. 10, A_1). Based on this value, the mean rate of horizontal movement over the late Pleistocene and Holocene is estimated at ~7.5 mm/yr, i.e., twice as low as the average for the Holocene. This estimate is apparently inaccurate, because the cumulative offset for 900 m was obtained by extrapolation of the shoreline angle segment trends of terrace MIS 5e from opposite sides of the fault at the base ~1.2 km (Figs. 3, 10). Pedoja et al. [40] estimated the right-lateral offsets of the shoreline angles of terraces t1 (MIS 5e, ~120000 years) and t2 (MIS 7, ~210000 years) at 1330 ± 40 m and 1350 ± 40 m; the mean rates have been estimated at 9.9 to 12 mm/yr and 5.7 to 7.3 mm/yr, respectively. These estimates also corroborate the acceleration of horizontal movements with time. It is noteworthy that the strike-slip offsets of the shoreline angles of terraces t1 and t2 (Fig. 10, A_1 and A_2) are approximately equal within the measurement accuracy limits. This implies that between the formation of these terraces from 210000 to 120000 years, the slip rate was close to zero or movements did not develop at all and resumed along the eastern fault segment only after the formation of terrace t1, i.e., since the end of the late Pleistocene.

The evident difference in the proportions of the horizontal and lateral components of movements along particular segments of the fault cannot be explained by the uncertainty of measurements. In the near-shore part of the fault, the rate of vertical movements is about 8 mm/yr, yielding only twice to the rate of horizontal movements, whereas far from the shore in the western segment of the fault, the rate of vertical movements is negligibly low as compared with horizontal movements. It remains unknown whether the proportion of horizontal and vertical components varies along the eastern segment of the fault. It can be inferred that the vertical component gradually decreases inland and approaches a value inherent to the western segment of the fault, or it remains constant and abruptly drops by passing from one fault segment to another. The first inference is consistent with distinct seaward tilt of top surface of elevations at an angle of ~3° in the northern side of the eastern segment of the fault, south of the Second Pereval'naya River (Fig. 3b), if it is actually a tectonic monocline. The second inference assumes that this tilt is a common primary seaward slope of marine terraces, so that depression bottom submerged with the same rate over the entire length. Both versions imply that larger vertical component of movements along the eastern segment of the fault is related to the formation of the basin now occupied by the Second Pereval'naya River valley and is not a property of the fault as a whole. The absence of significant vertical displacements along the eastern fault segment in the Quaternary is corroborated by approximately the same heights of tops of the near-meridional segment of the Kamchatsky Mys Range (Mount Komandnaya) and its near-latitudinal segment (Mount Africa) located to the north and south of the depression, respectively.

The mean rate of vertical movement in the eastern segment of the fault in the late Pleistocene–Holocene calculated by surface of the marine MIS 5e terrace is 2–3 mm/yr, i.e., 2.5–3.0 times lower than the rate calculated for the Holocene terrace (~8 mm/yr).

The total cumulative offset along the western part of the Second Pereval'naya River is estimated from the horizontal offset of the boundary of the territory occupied by the Ol'khovaya Formation. The eastern boundary is offset approximately 2.7 km, while the western boundary, approximately 1.3 km (Figs. 3; 10, A_3, A_4) in line with the westward decrease in the mean slip rate. The total horizontal offset along the eastern part of the fault, where movement started in late Pleistocene, is about 1 km. The lacking 2 km were apparently accommodated by slip along another, currently inactive fault. It is most probable that this fault was the northern boundary of uplifts in the Second Pereval'naya River valley. The projection of the eastern part of boundary of the Ol'khovaya Formation beneath loose sediments of the valley on this fault from the north gives offset from 1.3 to 1.8 km, which is close to the lacking offset. A maximum offset is reached, if a plan-view bend of the boundary near the fault is added to net offset (Fig. 10, A_5). Thus, it can be suggested that until the end of late Pleistocene, the Second Pereval'naya Fault on land consisted of two segments arranged en echelon and was afterward transformed into a single rectilinear fault. In general, the total $A_3 + A_5$ value of horizontal offset of the eastern boundary of the Ol'khovaya Formation along the active western part of the fault and the inactive fault to the north of the active eastern segment reached a maximum of 3.5 km. The extrapolation of shoreline segments and the submarine slope to the south and north of the Second Pereval'naya River (Fig. 10, A_6) gives a close value of the maximum cumulative offset (3.7–3.9 km). In the basin of the First Ol'khovaya River, i.e., in the northern side of the western fault segment, the Ol'khovaya Formation is represented by the upper subformation with the onset of deposition approximately 0.7–0.8 Ma ago [2]. This implies that the mean rate of strike-slip movements along the fault was approximately 4.5 mm/yr in the post-Ol'khovaya time.

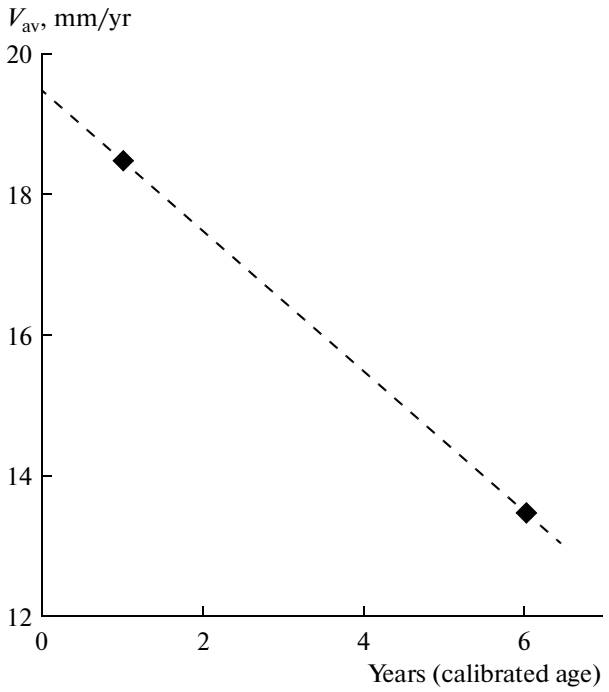

Fig. 11. Average slip rate (V) along Second Pereval'naya Fault over time intervals 0–2000 and 2000–10500 years (calibrated age)

The present-day rate of strike-slip movements along the Second Pereval'naya Fault can be approximately estimated by extrapolating the mean values for various time intervals of the Holocene to the present and assuming that within a short Holocene time interval, the relationship between them was linear (Fig. 11). The extrapolation result (~20 mm/yr) makes it possi-

ble to compare the obtained rates of strike-slip movements with the migration rate of GPS stations on the Kamchatsky Peninsula and Bering Island [14, 20] (Fig. 2c). If movement rate of Krutoberegovo station to the northwest (~15 mm/yr) is attributed to the northern side of the Second Pereval'naya Fault, then its southern side must move in the same direction at a rate of ~35 mm/yr. A difference between the rates of Krutoberegovo station and the southern side of the fault can be compensated, first, by the folding of the frontal (western) part of the southern side of the fault near the Pikezh and First Pereval'naya rivers, and second, by movement along the near-meridional fault zone, which conjugates in the north with the western end of the Second Pereval'naya Fault (Figs. 2c; 3a). The meridional fault zone on the western slope of the Kamchatsky Mys Range immediately to the east of the settlement of Krutoberegovo may be the westernmost element of this structural assembly. Combination of the right-lateral Second Pereval'naya Fault with the inferred near-meridional reverse–thrust fault system is similar to the reverse–strike-slip fault system in the westernmost part of the peninsula, which separates it from the rest of Kamchatka (Figs. 2; 3a).

The rates of westward movement of either the northern (15 mm/yr) or southern (35 mm/yr) sides of the Second Pereval'naya Fault are much lower than of the northwestern movement of the GPS station on Bering Island, i.e., of the Komandorsky Block (~50 mm/yr). A zone of shortening caused by this difference in rates can occur on the eastern continental slope of the peninsula, probably at the continental rise (Fig. 2c). Most likely, it should be compared with the zone of tectonic contact of the Aleutian arc and Kamchatsky Peninsula suggested from seismic data [29].

CONCLUSIONS

The horizontal movements along the Second Pereval'naya Fault in the Holocene were characterized by a high rate. For comparison, it can be seen that the mean rate over the last 2000 years (18–19 mm/yr) and the suggested modern rate (~20 mm/yr) are equal to the rate of horizontal movements in the Holocene along the North Anatolian Fault (18 ± 5 mm/yr) [30] and that it only slightly yields to the rate of movements along some segments of San Andreas Fault (24 ± 3 mm/yr) over the last 14000 years [37, 45]. The fast propagation of the southern side of the Second Pereval'naya Fault is apparently determined by the geodynamic situation, especially by the closeness to the contact of the western Aleutian arc and Pacific Plate as a source of motion. Comparison of the estimated rates of horizontal movements along the above fault and the rates of GPS station migration suggests that the southern side of the fault should be limited in the east and west by zones of horizontal shortening of the crust; i.e., it is a separate block (Fig. 2c). This implies, first, the possibility, to a certain degree, of independent movement of the southeastern part of the Kamchatsky Peninsula relative to the Komandorsky Block, and second, that the Second Pereval'naya River Fault is not an immediate onshore extension of the right-lateral Bering Fault on land.

From the two-thirds of the transform movement rate related to the northwestern drift of the western Aleutians, almost half is consumed by collisional deformation of the Kamchatsky Peninsula, which is a buffer in the zone of interaction between the Aleutian arc and Kamchatka. The remaining motions of the Komandorsky Block are apparently consumed by movements (probably underthrusting) in the zone of tectonic contact at the eastern continental slope of the peninsula established by Geist and Scholl [29].

The increase in mean rate of horizontal movements along the Second Pereval'naya River Fault reflects the acceleration of movement of the southern side of this fault (southeastern block of the Kamchatky Peninsula) since the onset of its motion in the early Quaternary.

ACKNOWLEDGMENTS

We thank M.V. Portnyagin (GEOMAR) for microprobe analyses of volcanic glasses. The study was supported by the Russian Foundation for Basic Research (projects nos. 11-05-00136-a, 12-05-00712-a, 11-05-98534-r_vostok_a).

REFERENCES

1. B. V. Baranov, C. Gaedicke, R. Freitag, and K. A. Dozorova, "Active faults of the southeastern Kamchatka Peninsula and Komandorsky Shear Zone," Vest. KRAUNTs, Nauki o Zemle **16**, No. 2, pp. 66–77 (2010).
2. A. E. Basilyan and M. E. Bylinskaya, "The shelf of the Kamchatsky Cape, eastern Kamchatka, in the late Pliocene and early Quaternary (Ol'khovaya time)," Stratigr. Geol. Correlation **5** (3), 281–289 (1997).
3. M. K. Bakhteev, O. A. Morozov, and S. R. Tikhomirova, "Paragenesis of structural elements in the junction zone of the Kurile–Kamchatka and Aleutian island arcs," Izv. Vyssh. Uchebn. Zaved., Geol. Razved., No. 3, 18–25 (1992).
4. *State Geological Map of the Russian Federation, Scale 1 : 200000, East Kamchatka Series, Map Sheets O-58-XXVI, -XXXI, -XXXII, Ust-Kamchatsk. Explanatory Notes*, 2nd ed. (VSEGEI, St. Petersburg, 2007) [in Russian].
5. V. P. Zenkovich, *Principles of Science on Development of Marine Shores* (USSR Acad. Sci., Moscow, 1962) [in Russian].
6. A. I. Kozhurin, "Young strike-slip faults in the Kumroch Range and Kamchatsky Mys Peninsula, East Kamchatka," Tikhookean. Geol. **9** (6), 45–55 (1990).
7. A. I. Kozhurin, "Quaternary tectonics of the Kumroch Range and Kamchatsky Mys Peninsula, East Kamchatka," Geotektonika **19** (2), 76–87 (1985).

8. A. I. Kozhurin and T. K. Pinegina, Active faulting of the Kamchatsky Mys Peninsula as manifestation of Kamchatka and Aleutian island arcs, in *Proceedings of the All-Russia Conference on Problems of Seismotectonics, September 20–24, 2011* (Inst. Physics Earth, Moscow, 2011), Vol. 4, pp. 260–263 [in Russian].
9. M. M. Pevzner, V. V. Ponomareva, and I. V. Melekestsev, "Cherny Yar, a reference section of Holocene key ashes at the northeastern shore of Kamchatka," Vulkanol. Seismol., No. 4, 3–18 (1997).
10. T. K. Pinegina, A. I. Kozhurin, and V. V. Ponomareva, "Estimation of seismic and thsunami hazard for Ust-Kamchatsk settlement (Kamchatka) from results of paleoseismological studies," Vestnik KRAUNTs, Nauki o Zemle, No. 1, 138–159 (2012).
11. T. K. Pinegina, E. A. Kravchunovskaya, A. V. Lander, A. I. Kozhurin, J. Bourgeois, and E. M. Martin, "Holocene vertical movements of the shore of Kamchatsky Mys Peninsula from the study of marine terraces," Vestnik KRAUNTs, Nauki o Zemle, No. 1, 100–116 (2010).
12. N. I. Seliverstov, "Structure of junction zone of the Kurile–Kamchatka and Aleutian island arcs from the data of continuous seismic profiling," Vulkanol. Seismol., No. 2, 53–67 (1983).
13. N. I. Seliverstov, V. M. Sugrobov, and F. A. Yanovsky, "Geological structure and evolution of the Komandorsky Basin from the results of Geophysical Research," Vulkanol. Seismol., No. 1, 38–53 (1995).
14. N. N. Titkov, V. F. Bakhtiarov, A. V. Lander, and V. A. Poletaev, "Estimation of deformation and displacement from the results of observation in the Kamchatka GPS network," in *Seismicity and Recent Geodynamics of the Far East and Eastern Siberia* (Inst. Tectonics Geophysics, Far East Branch, Russian Academy of Sciences, Khabarovsk, 2010), p. 312 [in Russian].
15. R. Arai, T. Iwasaki, H. Sato, S. Abe, and N. Hirata, "Collision and subduction structure of the Izu–Bonin arc, central Japan, revealed by refraction/wide-angle reflection analysis," Tectonophysics **475**, 438–453 (2009).
16. B. V. Baranov, N. I. Seliverstov, A. V. Muravev, and E. L. Muzurov, "The Komandorsky Basin as a product of spreading behind a transform plate boundary," Tectonophysics **199**, 237–269 (1991).
17. J. J. Becker, D. T. Sandwell, W. H. F. Smith, J. Braud, B. Binder, J. Depner, D. Fabre, J. Factor, S. Ingalls, S.-H. Kim, R. Ladner, K. Marks, S. Nelson, A. Pharaoh, G. Sharman, R. Trimmer, J. von Rosenburg, G. Wallace, and P. Weatherall, "Global bathymetry and elevation data at 30 arc seconds resolution: SRTM30_PLUS," Mar. Geod. **32** (4), 355–371 (2009).
18. J. Bourgeois, T. K. Pinegina, V. V. Ponomareva, and N. E. Zaretskaia, "Holocene tsunamis in the southwestern Bering Sea, Russian Far East and their tectonic implications," Geol. Soc. Amer. Bull. **11**, 449–463 (2006).
19. O. A. Braitseva, V. V. Ponomareva, L. D. Sulerzhitsky, and I. V. Melekestsev, and J. Bailey, "Holocene key-marker tephra layers in Kamchatka, Russia," Quaternary Res. **47**, 125–139 (1997).
20. R. Bürgmann, M. G. Kogan, G. M. Steblov, G. Hilley, and V. E. Levin, and E. Apel, "Interseismic coupling and asperity distribution along the Kamchatka subduction zone," J. Geophys. Res. **110**, No. B07405. doi: 10.1029/2005JB003648
21. V. F. Cormier, "Tectonics near the junction of the Aleutian and Kuril–Kamchatka arcs and a mechanism for middle Tertiary magmatism in the Kamchatka Basin," Geol. Soc. Amer. Bull. **86**, 443–453 (1975).
22. C. DeMets, "Oblique convergence and deformation along the Kuril and Japan trenches," J. Geophys. Res. **97**, 17615–17625 (1992).
23. C. DeMets and T. H. Dixon, "New kinematic models for Pacific–North America motion from 3 Ma to present, I: evidence of steady motion and biases in the NUVEL-1A model," Geophys. Rev. Lett. **26** (13), 1921–1924 (1999).
24. C. DeMets, R. G. Gordon, D. F. Argus, and S. Stein, "Effect of recent revisions of the geomagnetic reversal timescale on estimates of Curren Plate motions," Geophys. Rev. Lett. **21**, 2191–2194 (1994).
25. C. DeMets, R. G. Gordon, D. F. Argus, and S. Stein, "Current plate motions," Geophys. J. Int. **101**, 425–478 (1990).
26. T. J. Fitch, "Plate convergence, transcurrent faults, and internal deformation adjacent to southeast Asia and the western Pacific," J. Geophys. Res. **77**, 4432–4460 (1972).
27. R. Freitag, C. Gaedicke, B. Baranov, and N. Tsukanov, "Collisional processes at the junction of the Aleutian–Kamchatka arcs: new evidence from fission track analysis and field observations," Terra Nova **13**, 433–442 (2001).
28. C. Gaedicke, B. Baranov, N. Seliverstov, D. Alexeiev, N. Tsukanov, and R. Freitag, "Structure of an active arc–continent collision area: the Aleutian–Kamchatka junction," Tectonophysics **325**, 63–85 (2000).
29. E. L. Geist and D. W. Scholl, "Large-scale deformation related to the collision of the Aleutian arc with Kamchatka," Tectonics **13**, 538–560 (1994).
30. A. Hubert-Ferrari, R. Armijo, G. King, and B. Meyer, "Morphology, displacement, and slip rates along the North Anatolian Fault, Turkey," J. Geophys. Res. **107** (B10), ETG 9-1–9.33.223. (2002). doi: 10.1029/2001JB000393
31. T. Ito, "Active faulting, lower crustal delamination and ongoing Hidaka arc–arc collision, Hokkaido, Japan," in *Seismotectonics in Convergent Plate Boundary*, Ed. by Y. Fujinawa and A. Yoshida (TERRAPUB, Tokio, 2002), pp. 219–224.
32. G. Kimura, "Collision orogeny at arc–arc junctions in the Japanese Islands," The Island Arc, No. 5, 262–275 (1996).
33. G. Kimura, "Oblique subduction and collision: Forearc tectonics of the Kuril Arc," Geology **14**, 404–407 (1986).
34. A. I. Kozhurin, "Active faulting in the Kamchatsky Mys Peninsula, Kamchatka–Aleutian junction," In *Volcanism and Subduction: The Kamchatka Region* (AGU Geophys. Monograph Series, 2007), Vol. 172, pp. 263–282.

35. A. I. Kozhurin, V. Acocella, P. R. Kyle, et al., "Trenching studies of active faults in Kamchatka, eastern Russia: paleoseismic, tectonic and hazard implications," Tectonophysics **417**, 285–304 (2006).

36. D. J. Lowe, "Tephrochronology and its application: A review," Quat. Geochronol. **6**, 107–153 (2011).

37. T. N. Niemi and N. T. Hall, "Late Holocene slip rate and recurrence of great earthquakes on the San Andreas Fault in northern California," Geol. Soc. Amer. Bull. **20** (3), 195–198 (1992).

38. *Paleoseismology*, 1st ed., Ed. by J. P. McCalpin (Elsevier, 1996).

39. *Paleoseismology,* 2nd ed., Ed. by J. P. McCalpin (Academic Press, 2009).

40. K. Pedoja, C. Authemayou, T. Pinegina, J. Bourgeois, M. Nexer, B. Delcaillau, and V. Regard, "Arc-continent collision" of the Aleutian–Komandorsky arc into Kamchatka: insight into Quaternary tectonic segmentation through Pleistocene marine terraces and morphometric analysis of fluvial drainage," Tectonics **32** (4), 821–1025 (2013). doi: 10.1002/tect.20051

41. K. Pedoja, J. Bourgeois, T. Pinegina, and B. Higman, "Does Kamchatka belong to North America? An extruding Okhotsk Block suggested by coastal neotectonics of the Ozernoi Peninsula, Kamchatka, Russia," Geology **34** (5), 353–356 (2006).

42. T. K. Pinegina, J. Bourgeois, E. A. Kravchunovskaya, A. V. Lander, M. E. M. Arcos, and K. Pedoja, and B. T. MacInnes, "A nexus of plate interaction: segmented vertical movement of Kamchatsky Mys Peninsula (Kamchatka) based on Holocene aggradational marine terraces," Geol. Soc. Amer. Bull. **125** (9/10), 1554–1568 (2013). doi: 10.1130/B30793.1

43. V. Ponomareva, M. Portnyagin, A. Derkachev, I. F. Pendea, J. Bourgeois, P. J. Reimer, D. Garbe-Schönberg, S. Krasheninnikov, and D. Nürnberg, "Early Holocene M ~ 6 explosive eruption from Plosky volcanic massif (Kamchatka) and its tephra as a link between terrestrial and marine paleoenvironmental records," Int. J. Earth Sci. **102** (6), 1673–1699 (2013). doi: 10.1007/s00531-013-0898-0

44. G. F. Sella, T. H. Dixon, and A. Mao, "REVEL: A model for recent plate rates from space geodesy," J. Geophys. Res.: Solid Earth **107** (B4), ETG 11-1–ETG 11-30 (2002).

45. K. E. Sieh, "Holocene rate of slip and tentative recurrence interval for large earthquakes on the San Andreas Fault, Cajon Pass, southern California," Geol. Soc. Amer. Bull. **96** (6), 793–812 (1985).

46. H. Yamazaki, "Tectonics of a plate collision along the northern margin of Izu Peninsula, Central Japan," Bull. Geol. Soc. Japan **43** (10), 603–657 (1992).

Reviewers: E.A. Rogozhin and A.V. Solov'ev